Computers & Structures Vol. 15, No. 2, pp. 177–183, 1982
Printed in Great Britain.

0045-7949/82/020177–07$03.00/0


# A REFINED HIGHER-ORDER $C^0$ PLATE BENDING ELEMENT

TARUN KANT†
Department of Civil Engineering, Indian Institute of Technology, Bombay 400 076, India

and

D. R. J. OWEN‡ and O. C. ZIENKIEWICZ§
Department of Civil Engineering, University of Wales, University College of Swansea, Swansea SA2 8PP, Wales

(*Received* 2 *December* 1980; *received for publication* 20 *January* 1981)

**Abstract**—A general finite element formulation for plate bending problem based on a higher-order displacement model and a three-dimensional state of stress and strain is attempted. The theory incorporates linear and quadratic variations of transverse normal strain and transverse shearing strains and stresses respectively through the thickness of the plate. The 9-noded quadrilateral from the family of two dimensional $C^0$ continuous isoparametric elements is then introduced and its performance is evaluated for a wide range of plates under uniformly distributed load and with different support conditions and ranging from very thick to extremely thin situations. The effect of full, reduced and selective integration schemes on the final numerical result is examined. The behaviour of this element with the present formulation is seen to be excellent under all the three integration schemes.

## INTRODUCTION

Isoparametric plate elements[1–5] based on Mindlin's theory[6], which obviate most of the problems that beset elements based on the classical Kirchhoff's plate theory[7], have become popular and well established. However the theory itself has certain limitations, viz., the effects of transverse normal strain and transverse normal stress are not accounted for, the transverse shearing strains are assumed constant through the thickness and a fictitious shear correction coefficient is introduced to account for warping of the cross-section. Thus the claim that the element is applicable to both thin and thick plates is not tenable. At the most only moderately thick plates could be analysed. In this paper a $C^0$ continuity element is developed based on a higher-order displacement model than hitherto used and a three dimensional state of stress and strain[8, 9]. Specifically, the transverse normal strain and the transverse shearing strains are now assumed to vary linearly and quadratically respectively through the thickness of the plate. Thus the warping of the cross-section is automatically incorporated. This element retains the simplicity of Mindlin's formulation and, at the same time, has no intrinsic limitations. It is expected that this development will offer refined and realistic solutions in the case of really thick situations in general, and composite/layered systems, stress-distribution near concentrated loads, etc. in particular. The element which has six degrees of freedom per node can employ the available family of the Serendipity and the Lagrange elements[5, 10]. In the present study a 9-noded Lagrange quadrilateral is used which has performed very well on all of the test problems. Numerical results corresponding to exact, reduced and selective integrations for a wide spectrum of plates—very thick to extremely thin—are presented.

## ELEMENT FORMULATION

The general theory[8, 9] is based on the displacement model (Fig. 1)

$$\mathbf{u} = \begin{bmatrix} U(x, y, z) = z\theta_x(x, y) + z^3\theta_x^*(x, y) \\ V(x, y, z) = z\theta_y(x, y) + z^3\theta_y^*(x, y) \\ W(x, y, z) = w(x, y) + z^2 w^*(x, y) \end{bmatrix} \quad (1)¶$$

where $U$, $V$ and $W$ define the displacement components in the coordinate directions $x$, $y$ and $z$ respectively. Both the $x$ and $y$ coordinates lie in the reference plane of the plate which is assumed unstrained. The terms $\theta_x$ and $\theta_y$ are the usual average rotations of the normals to the reference plane along the $x$ and $y$ directions respectively, while $w$ defines the transverse displacement at the reference surface. The terms $\theta_x^*$, $\theta_y^*$ and $w^*$ are the corresponding higher-order terms in the Taylor's series expansion used in the present theory and are also defined at the reference plane. Thus the generalized displace-

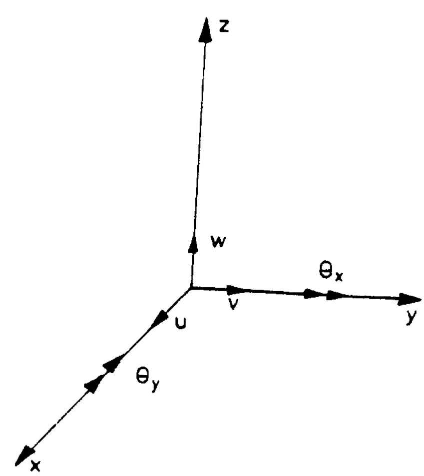


Fig. 1. Positive set of displacement components.

†Assistant Professor, presently a Visitor in the Department of Civil Engineering, University of Wales, University College Swansea, Swansea SA2, 8PP, Wales, under the Jawaharlal Nehru Memorial Trust (U.K.) Scholarship 1979 Award.

‡Reader.

§Professor and Head of Department.

¶$U(x, y, z)$, $\theta_x(x, y)$, $w^*(x, y)$, etc. will henceforth be written simply as $U$, $\theta_x$, $w^*$, etc.

ment of the reference plane $\delta$ is expressed in terms of six independent variables,

$$\delta = [w, \theta_x, \theta_y, w^*, \theta_x^*, \theta_y^*]^T. \tag{2}$$

The six three dimensional strain components are then related to the generalised displacement components $\delta$ by the relation,

$$\begin{aligned} \epsilon_x &= zK_x + z^3K_x^* \\ \epsilon_y &= zK_y + z^3K_y^* \\ \gamma_{xy} &= zK_{xy} + z^3K_{xy}^* \\ \gamma_{xz} &= \phi_x + z^2\phi_x^* \\ \gamma_{yz} &= \phi_y + z^2\phi_y^* \\ \epsilon_z &= 2zw^* \end{aligned} \tag{3}$$

where the new curvature terms $K_x$, $K_y$, etc. called the generalised strain components vector $\epsilon$ in the two dimensional finite element context, are related to the generalised displacement components $\delta$ by the following matrix relation.

$$\epsilon = \begin{Bmatrix} K_x \\ K_y \\ K_{xy} \\ \phi_x \\ \phi_y \\ K_x^* \\ K_y^* \\ K_{xy}^* \\ \phi_x^* \\ \phi_y^* \\ 2w^* \end{Bmatrix} = \begin{bmatrix} 0 & \frac{\partial}{\partial x} & 0 & 0 & 0 & 0 \\ 0 & 0 & \frac{\partial}{\partial y} & 0 & 0 & 0 \\ 0 & \frac{\partial}{\partial y} & \frac{\partial}{\partial x} & 0 & 0 & 0 \\ \frac{\partial}{\partial x} & 1 & 0 & 0 & 0 & 0 \\ \frac{\partial}{\partial y} & 0 & 1 & 0 & 0 & 0 \\ 0 & 0 & 0 & 0 & \frac{\partial}{\partial x} & 0 \\ 0 & 0 & 0 & 0 & 0 & \frac{\partial}{\partial y} \\ 0 & 0 & 0 & 0 & \frac{\partial}{\partial y} & \frac{\partial}{\partial x} \\ 0 & 0 & 0 & \frac{\partial}{\partial x} & 3 & 0 \\ 0 & 0 & 0 & \frac{\partial}{\partial y} & 0 & 3 \\ 0 & 0 & 0 & 2 & 0 & 0 \end{bmatrix} \begin{Bmatrix} w \\ \theta_x \\ \theta_y \\ w^* \\ \theta_x^* \\ \theta_y^* \end{Bmatrix} = \underset{\sim}{L}\delta \tag{4}$$

The total potential energy $\pi$ for the present theory[9] is given by

$$\pi = \frac{1}{2}\int_A \epsilon^T\sigma \,\mathrm{d}A - \int_A (p_z^+ + p_z^-)\left(w + \frac{h^2}{4}w^*\right)\mathrm{d}A \tag{5}$$

where $p_z^+$ and $p_z^-$ are the transverse distributed loads on the positive and negative extreme $z$ planes respectively and $h$ is the total thickness of the plate. The generalised stress component vector $\sigma$ which is the integral of the physical stress components through the thickness of the plate (see Ref. [9] and Figs. 2–4) is given by

$$\sigma = [M_x, M_y, M_{xy}, Q_x, Q_y, M_x^*, M_y^*, M_{xy}^*, Q_x^*, Q_y^*, M_z]^T. \tag{6}$$

The generalized stress vector $\sigma$ and the generalised strain vector $\epsilon$ are partitioned as follows:

$$\sigma = [\sigma_{b1}, \sigma_{s1}, \sigma_{b2}, \sigma_{s2}, \sigma_{b3}]^T \tag{7}$$

and

$$\epsilon = [\epsilon_{b1}, \epsilon_{s1}, \epsilon_{b2}, \epsilon_{s2}, \epsilon_{b3}]^T \tag{8}$$

where

$$\begin{aligned} &\sigma_{b1} = [M_x, M_y, M_{xy}]^T, \ \sigma_{b2} = [M_x^*, M_y^*, M_{xy}^*]^T, \\ &\sigma_{b3} = M_z, \ \sigma_{s1} = [Q_x, Q_y]^T, \ \sigma_{s2} = [Q_x^*, Q_y^*]^T, \\ &\epsilon_{b1} = [K_x, K_y, K_{xy}]^T, \ \epsilon_{b2} = [K_x^*, K_y^*, K_{xy}^*]^T, \\ &\epsilon_{b3} = 2w^*, \ \epsilon_{s1} = [\phi_x, \phi_y]^T, \ \epsilon_{s2} = [\phi_x^*, \phi_y^*]^T. \end{aligned} \tag{9}$$

For a linear elastic material the constitutive relation can be written as

$$\sigma_{b1} = \underset{\sim}{D}_{b1}\epsilon_{b1} + \underset{\sim}{D}_{b2}\epsilon_{b2} + \underset{\sim}{D}_{b3}\cdot 2w^* \tag{10a}$$

$$\sigma_{b2} = \underset{\sim}{D}_{b2}\epsilon_{b1} + \underset{\sim}{D}_{b4}\epsilon_{b2} + \underset{\sim}{D}_{b5}\cdot 2w^* \tag{10b}$$

$$\sigma_{b3} = \underset{\sim}{D}_{b3}^T\epsilon_{b1} + \underset{\sim}{D}_{b5}^T\epsilon_{b2} + \underset{\sim}{D}_{b6}\cdot 2w^* \tag{10c}$$

$$\sigma_{s1} = \underset{\sim}{D}_{s1}\epsilon_{s1} + \underset{\sim}{D}_{s2}\epsilon_{s2} \tag{10d}$$

$$\sigma_{s2} = \underset{\sim}{D}_{s2}\epsilon_{s1} + \underset{\sim}{D}_{s3}\epsilon_{s2} \tag{10e}$$

where the elasticity matrices $\underset{\sim}{D}_{b1}$, $\underset{\sim}{D}_{b2}$, $\underset{\sim}{D}_{s1}$, $\underset{\sim}{D}_{s2}$, etc. for a homogeneous and isotropic plate with Young's modulus $E$, Poisson's ratio $\nu$ and thickness $h$ are expressed in the following manner:

$$\underset{\sim}{D}_{b1} = \frac{Eh^3}{12(1+\nu)(1-2\nu)}\begin{bmatrix} 1-\nu & \nu & 0 \\ \nu & 1-\nu & 0 \\ 0 & 0 & \frac{1-2\nu}{2} \end{bmatrix} \tag{11a}$$

$$\underset{\sim}{D}_{b2} = \frac{Eh^5}{80(1+\nu)(1-2\nu)}\begin{bmatrix} 1-\nu & \nu & 0 \\ \nu & 1-\nu & 0 \\ 0 & 0 & \frac{1-2\nu}{2} \end{bmatrix} \tag{11b}$$

$$\underset{\sim}{D}_{b3} = \frac{Eh^3}{12(1+\nu)(1-2\nu)}\begin{Bmatrix} \nu \\ \nu \\ 0 \end{Bmatrix} \tag{11c}$$

$$\underset{\sim}{D}_{b4} = \frac{Eh^7}{448(1+\nu)(1-2\nu)}\begin{bmatrix} 1-\nu & \nu & 0 \\ \nu & 1-\nu & 0 \\ 0 & 0 & \frac{1-2\nu}{2} \end{bmatrix} \tag{11d}$$

$$\underset{\sim}{D}_{b5} = \frac{Eh^5}{80(1+\nu)(1-2\nu)}\begin{Bmatrix} \nu \\ \nu \\ 0 \end{Bmatrix} \tag{11e}$$

$$\underset{\sim}{D}_{b6} = \frac{Eh^3}{12(1+\nu)(1-2\nu)}(1-\nu) \tag{11f}$$

$$\underset{\sim}{D}_{s1} = \frac{Eh}{2(1+\nu)}\begin{bmatrix} 1 & 0 \\ 0 & 1 \end{bmatrix} \tag{11g}$$

$$\underset{\sim}{D}_{s2} = \frac{Eh^3}{24(1+\nu)}\begin{bmatrix} 1 & 0 \\ 0 & 1 \end{bmatrix} \tag{11h}$$

$$\underset{\sim}{D}_{s3} = \frac{Eh^5}{160(1+\nu)}\begin{bmatrix} 1 & 0 \\ 0 & 1 \end{bmatrix}. \tag{11i}$$

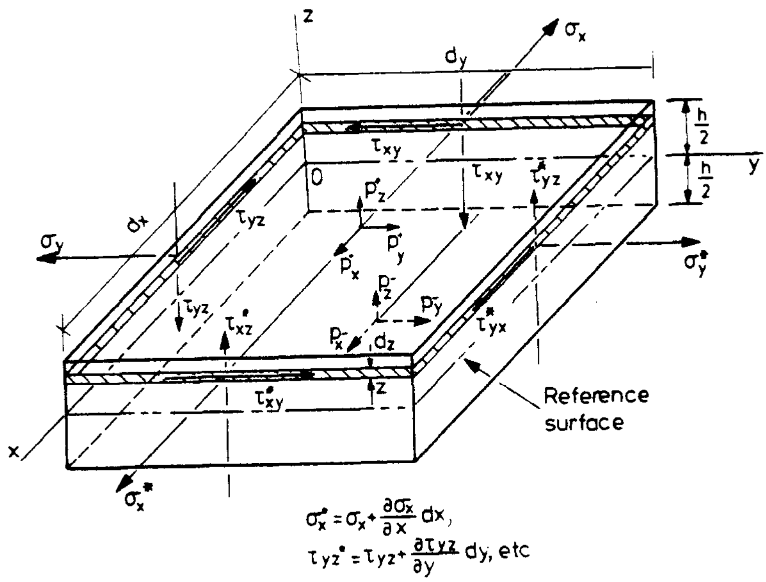


Fig. 2. Positive set of stress components.

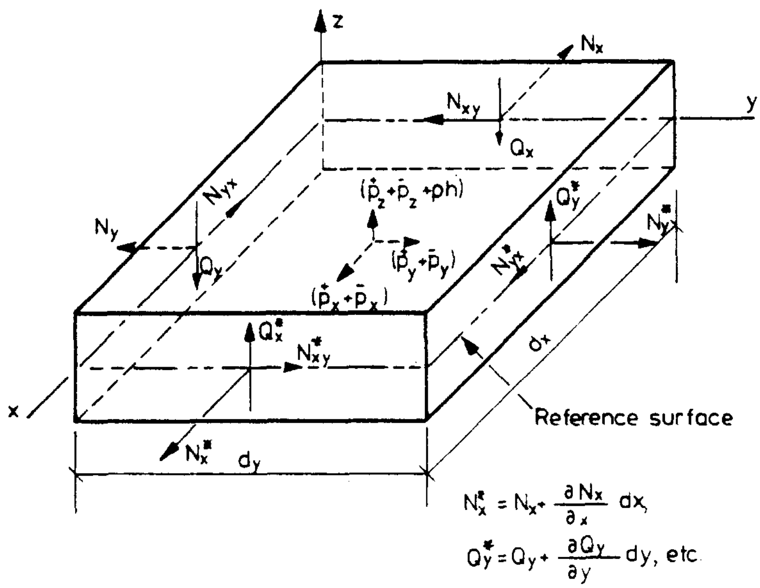


Fig. 3. Positive set of stress resultants-forces.

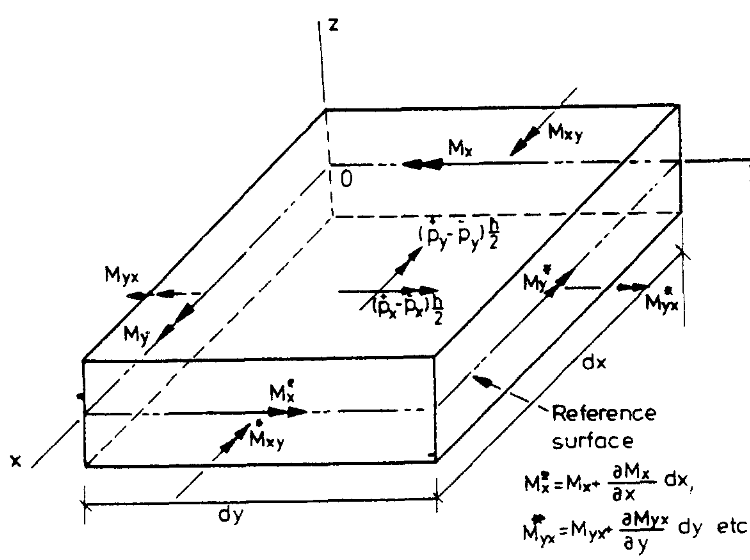


Fig. 4. Positive set of stress resultants-couples.

It is seen that the strain energy expression of eqn (5) contains only the first derivatives of the components of the generalized displacement vector $\delta$ and thus only $C^0$ continuity is required for the shape functions to be used in the element formulation. If the same shape function is used to define all the components of the generalized displacement vector $\delta$, then

$$\delta = \sum_{i=1}^{m} N_i \delta_i \tag{12}$$

where $N_i$ is the shape function associated with node $i$, $\delta_i$ is the value of $\delta$ corresponding to node $i$ and $m$ is the number of nodes in the element.

With the generalized displacement vector $\delta$ known at all points within the element, the generalized strain vector $\epsilon$ at any point is determined with the aid of eqns (4) and (12), as follows:

$$\epsilon = \underset{\sim}{L}\delta = \underset{\sim}{L} \sum_{i=1}^{m} N_i \delta_i = \sum_{i=1}^{m} \underset{\sim}{B}_i \delta_i \tag{13}$$

where

$$\underset{\sim}{B}_i = \underset{\sim}{L} N_i \tag{14}$$

and is given explicitly for the present case as follows:

$$\underset{\sim}{B}_i = \begin{bmatrix} 0 & \frac{\partial}{\partial x} & 0 & 0 & 0 & 0 \\ 0 & 0 & \frac{\partial}{\partial y} & 0 & 0 & 0 \\ 0 & \frac{\partial}{\partial y} & \frac{\partial}{\partial x} & 0 & 0 & 0 \\ \frac{\partial}{\partial x} & 1 & 0 & 0 & 0 & 0 \\ \frac{\partial}{\partial y} & 0 & 1 & 0 & 0 & 0 \\ 0 & 0 & 0 & 0 & \frac{\partial}{\partial x} & 0 \\ 0 & 0 & 0 & 0 & 0 & \frac{\partial}{\partial y} \\ 0 & 0 & 0 & 0 & \frac{\partial}{\partial y} & \frac{\partial}{\partial x} \\ 0 & 0 & 0 & \frac{\partial}{\partial x} & 3 & 0 \\ 0 & 0 & 0 & \frac{\partial}{\partial y} & 0 & 3 \\ 0 & 0 & 0 & 2 & 0 & 0 \end{bmatrix} N_i. \tag{15}$$

Having obtained the $\underset{\sim}{D}$ and $\underset{\sim}{B}$ matrices as given by eqns (11) and (15) respectively the element stiffness matrix $\underset{\sim}{D}^e$ can be conveniently expressed in the following form[10]:

$$\underset{\sim}{K}^e = \int_{A^e} \underset{\sim}{B}^T \underset{\sim}{D} \underset{\sim}{B} \, dA = \int_{-1}^{+1} \int_{-1}^{+1} \underset{\sim}{B}^T \underset{\sim}{D} \underset{\sim}{B} |\underset{\sim}{J}| \, d\xi \, d\eta \tag{16}$$

For the present element which has six degrees of freedom per node as opposed to Mindlin's element[1, 10] which has only three degrees of freedom per node, it is considered appropriate to economise on the cost of computation involved in numerical quadrature for evaluating the integral in eqn (16). It is generally agreed that the foregoing computation accounts for a very substantial part of the total computation cost of the complete analysis[11]. To achieve this end, the element stiffness matrix is partitioned in both the row and column directions into blocks. Each block corresponds to the degrees of freedom at a node[12]. The expression of the stiffness coefficients for a typical block $ij$ could be written as follows:

$$\underset{\sim}{K}^{ij} = \sum_{p=1}^{n} \sum_{q=1}^{n} W_p W_q |\underset{\sim}{J}| \underset{\sim}{B}_i^T \underset{\sim}{D} \underset{\sim}{B}_j \tag{17}$$

where $W_p$ and $W_q$ are weighting coefficients, $n$ is the number of numerical quadrature points in each direction and $\underset{\sim}{B}_i$ and $\underset{\sim}{B}_j$ are the strain-displacement matrices based on the $i$th and $j$th shape functions, respectively. Due to symmetry of the stiffness matrix $\underset{\sim}{K}^e$, only the blocks $\underset{\sim}{K}^{ij}$ lying on one side of the main diagonal are formed (Fig. 5). Further, the suggestion of Gupta[13] is incorporated in the program which stipulates explicit multiplication of the $\underset{\sim}{B}_i$, $\underset{\sim}{D}$ and $\underset{\sim}{B}_j$ matrices instead of carrying out the full matrix multiplication of the triple product. This is expected to reduce the computing time for element stiffness formulation by a factor of nine. For the convenience of any prospective user, these $6 \times 6$ submatrices corresponding to flexure and transverse shear effects are presented in Appendix 1.

The consistent load vector **P** due to distributed load **p** can be written in general as:

$$\mathbf{P} = \int_{A^e} \mathbf{N}^T \mathbf{p} \, dA = \int_{-1}^{+1} \int_{-1}^{+1} \mathbf{N}^T \mathbf{p} |\underset{\sim}{J}| \, d\xi \, d\eta \tag{18}$$

which takes the following form suitable for numerical integration when transformed in the context of the energy expression (5) for the theory presented in this paper

$$\mathbf{P} = \sum_{p=1}^{n} \sum_{q=1}^{n} W_p W_q |\underset{\sim}{J}| N_i \begin{Bmatrix} 1 \\ 0 \\ 0 \\ h^2/4 \\ 0 \\ 0 \end{Bmatrix} (p_z^+ + p_z^-). \tag{19}$$

It is noted that eqn (19) is different from the usual ones because the loads are not assumed to act on the reference surface in the present development.

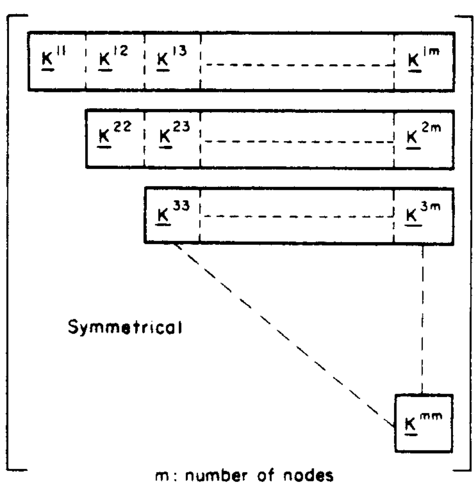


Fig. 5. Nodal partitions of the element stiffness matrix.

A computer program was developed based on the foregoing approach to generate the element stiffness matrices, the consistent load vector and a few related processes for the stress computation. This program was integrated with the modified version of the one described in detail by Hinton and Owen[14].

## NUMERICAL EXAMPLES

A square plate of side $a = 1$ and subjected to a transverse distributed load $p_z = 1$ is analysed with three types of boundary conditions. A Poisson's ratio ($\nu$) of 0.3 is assumed. The numerical experimentation is carried out with four of the nine noded Lagrangian quadrilateral elements in a quarter plate. All the computations were performed on a CDC 7600 computer in single precision with 14 significant digits of real rounded arithmetic accuracy. Full, reduced and selective integration schemes based on Gauss-Legendre product rules, viz. $3\times3$ and $3\times3(E)$, $2\times2$ and $2\times2(R)$ and $3\times3$ and $2\times2(S)$, have been employed for flexure and shear contributions respectively to the element stiffness matrix computation. The results for the plate analysed with the three boundary conditions are presented in Tables 1–3 for various values of the aspect ratio $a/h$. Typical execution time is 0.52 CP seconds per analysis.

## CONCLUSIONS

The performance of the 9-noded Lagrangian isoparametric element has been studied in conjunction with the refined higher-order plate theory presented in this paper—and also elsewhere[8,9]. On the basis of the results of Tables 1–3 it can be positively concluded that the element's performance is excellent in all the situations studied in this paper with no apparent preferential choice for full (exact), reduced and selective integration schemes for computation of the element stiffness matrix[1–5, 15, 16]. This appears to be very significant and perhaps is a pointer towards the use of the present refined higher-order theory in preference to Mindlin theory hitherto used in most of the analyses. Qualitatively this could be due to the better representations of the cross-sectional deformations and the stress-strain law. However, its behaviour in context of the few boundary constraints which lead to the development of mechanisms (or near mechanisms) commonly interpreted as zero energy modes[5] needs to be seen.

## REFERENCES


1. E. Hinton, A. Razzaque, O. C. Zienkiewicz and J. D. Davies, Simple finite element solution for plates of homogeneous, sandwich and cellular construction. *Proc. of the Institution of Civil Engineers, Part II*, **59**, 43–65 (1975).
2. T. J. R. Hughes, R. L. Taylor and W. Kanoknukulchai, A simple and efficient finite element for plate bending. *Int. J. Num. Meth. Engng.* **11**, 1529–1543 (1977).
3. E. D. L. Pugh, E. Hinton and O. C. Zienkiewicz, A study of quadrilateral plate bending elements with reduced integration. *Int. J. Num. Meth. Engng.* **12**, 1059–1079 (1978).


Table 1. Simply supported square plate under uniform loading with $w = \theta_t = w^* = \theta_t^* = 0(s)$ along its four edges

| a/h | Integ. Type | Central Displacement $*pa^4/D$ | Central$^+$ Bending Moment $*pa^2$ | Corner$^+$ Twisting Moment $*pa^2$ | Mid-edge$^+$ Shear Force $*pa$ |
|---|---|---|---|---|---|
| | E | 0.00853 | 0.0521 | - 0.0223 | 0.311 |
| 2 | R | 0.00854 | 0.0509 | - 0.0216 | 0.285 |
| | S | 0.00854 | 0.0522 | - 0.0219 | 0.285 |
| | E | 0.00612 | 0.0499 | - 0.0276 | 0.315 |
| 3 | R | 0.00612 | 0.0488 | - 0.0262 | 0.285 |
| | S | 0.00611 | 0.0500 | - 0.0272 | 0.285 |
| | E | 0.00522 | 0.0491 | - 0.0295 | 0.322 |
| 4 | R | 0.00523 | 0.0480 | - 0.0279 | 0.285 |
| | S | 0.00523 | 0.0492 | - 0.0292 | 0.285 |
| | E | 0.00480 | 0.0487 | - 0.0304 | 0.330 |
| 5 | R | 0.00482 | 0.0477 | - 0.0287 | 0.285 |
| | S | 0.00481 | 0.0488 | - 0.0302 | 0.285 |
| | E | 0.00423 | 0.0480 | - 0.0315 | 0.381 |
| 10 | R | 0.00426 | 0.0472 | - 0.0299 | 0.285 |
| | S | 0.00426 | 0.0484 | - 0.0314 | 0.285 |
| | | (0.00427 Exact) | | | |
| | E | 0.00398 | 0.0470 | - 0.0317 | 0.573 |
| 50 | R | 0.00408 | 0.0471 | - 0.0302 | 0.285 |
| | S | 0.00408 | 0.0482 | - 0.0319 | 0.285 |
| | E | 0.00397 | 0.0469 | - 0.0317 | 0.597 |
| 100 | R | 0.00407 | 0.0471 | - 0.0302 | 0.285 |
| | S | 0.00407 | 0.0482 | - 0.0319 | 0.284 |
| | E | 0.00396 | 0.0468 | - 0.0317 | 0.606 |
| 1000 | R | 0.00407 | 0.0471 | - 0.0302 | 0.285 |
| | S | 0.00407 | 0.0482 | - 0.0319 | 0.284 |
| | E | 0.00396 | 0.0468 | - 0.0317 | 0.606 |
| 10000 | R | 0.00407 | 0.0471 | - 0.0302 | 0.285 |
| | S | 0.00407 | 0.0482 | - 0.0319 | 0.284 |
| ( )$^{++}$ | | 0.00406 | 0.0479 | - 0.0325 | 0.338 |

$^+$ Values at nearest Gauss point

$^{++}$ Classical thin plate solution (Ref. 7)

Table 2. Simply supported square plate under uniform loading with $w = w^* = 0(s^*)$ along its four edges

| a/h | Integ. Type | Central Displacement *pa⁴/D | Central[+] Bending Moment *pa² | Corner[+] Twisting Moment *pa² | Mid-edge[+] Shear Force *pa |
|---|---|---|---|---|---|
| 2 | E | 0.00949 | 0.0602 | - 0.00208 | 0.324 |
| | R | 0.00944 | 0.0596 | - 0.00302 | 0.301 |
| | S | 0.00943 | 0.0605 | - 0.00095 | 0.301 |
| 3 | E | 0.00695 | 0.0573 | - 0.00509 | 0.336 |
| | R | 0.00693 | 0.0568 | - 0.00545 | 0.310 |
| | S | 0.00693 | 0.0577 | - 0.00337 | 0.309 |
| 4 | E | 0.00592 | 0.0552 | - 0.00789 | 0.345 |
| | R | 0.00593 | 0.0548 | - 0.00751 | 0.314 |
| | S | 0.00592 | 0.0558 | - 0.00538 | 0.312 |
| 5 | E | 0.00538 | 0.0538 | - 0.01051 | 0.353 |
| | R | 0.00541 | 0.0534 | - 0.00928 | 0.316 |
| | S | 0.00540 | 0.0546 | - 0.00716 | 0.313 |
| 10 | E | 0.00448 | 0.0503 | - 0.0200 | 0.397 |
| | R | 0.00458 | 0.0503 | - 0.0152 | 0.322 |
| | S | 0.00458 | 0.0521 | - 0.0135 | 0.318 |
| 50 | E | 0.00400 | 0.0472 | - 0.0308 | 0.561 |
| | R | 0.00419 | 0.0483 | - 0.0218 | 0.341 |
| | S | 0.00420 | 0.0511 | - 0.0216 | 0.339 |
| 100 | E | 0.00397 | 0.0469 | - 0.0314 | 0.583 |
| | R | 0.00418 | 0.0482 | - 0.0221 | 0.343 |
| | S | 0.00418 | 0.0511 | - 0.0221 | 0.341 |
| 1000 | E | 0.00396 | 0.0468 | - 0.0317 | 0.591 |
| | R | 0.00417 | 0.0481 | - 0.0223 | 0.344 |
| | S | 0.00417 | 0.0511 | - 0.0223 | 0.342 |
| 10000 | E | 0.00396 | 0.0468 | - 0.0317 | 0.591 |
| | R | 0.00417 | 0.0481 | - 0.0223 | 0.344 |
| | S | 0.00417 | 0.0511 | - 0.0223 | 0.342 |

[+]Values at nearest Gauss point.

Table 3. Clamped square plate under uniform loading with $w = \theta_n = \theta_t = w^* = \theta_n^* = \theta_t^* = 0(c)$ along its four edges

| a/h | Integ. Type | Central Displacement *pa⁴/D | Central[+] Bending Moment *pa² | Mid-Edge[+] Bending Moment *pa² | Mid-edge[+] Shear Force *pa |
|---|---|---|---|---|---|
| 2 | E | 0.00607 | 0.0335 | - 0.0262 | 0.332 |
| | R | 0.00611 | 0.0320 | - 0.0190 | 0.297 |
| | S | 0.00609 | 0.0338 | - 0.0267 | 0.297 |
| 3 | E | 0.00349 | 0.0283 | - 0.0309 | 0.352 |
| | R | 0.00355 | 0.0270 | - 0.0242 | 0.306 |
| | S | 0.00352 | 0.0287 | - 0.0319 | 0.306 |
| 4 | E | 0.00253 | 0.0261 | - 0.0329 | 0.374 |
| | R | 0.00261 | 0.0252 | - 0.0264 | 0.315 |
| | S | 0.00256 | 0.0267 | - 0.0344 | 0.315 |
| 5 | E | 0.00206 | 0.0250 | - 0.0337 | 0.398 |
| | R | 0.00216 | 0.0243 | - 0.0277 | 0.323 |
| | S | 0.00211 | 0.0256 | - 0.0359 | 0.323 |
| 10 | E | 0.00138 | 0.0228 | - 0.0327 | 0.518 |
| | R | 0.00152 | 0.0228 | - 0.0299 | 0.344 |
| | S | 0.00146 | 0.0236 | - 0.0387 | 0.344 |
| 50 | E | 0.00100 | 0.0207 | - 0.0194 | 0.906 |
| | R | 0.00129 | 0.0222 | - 0.0308 | 0.356 |
| | S | 0.00123 | 0.0227 | - 0.0399 | 0.356 |
| 100 | E | 0.00097 | 0.0205 | - 0.0177 | 0.956 |
| | R | 0.00128 | 0.0222 | - 0.0308 | 0.357 |
| | S | 0.00123 | 0.0227 | - 0.0399 | 0.356 |
| 1000 | E | 0.00096 | 0.0204 | - 0.0170 | 0.975 |
| | R | 0.00128 | 0.0222 | - 0.0308 | 0.357 |
| | S | 0.00122 | 0.0227 | - 0.0399 | 0.356 |
| 10000 | E | 0.00096 | 0.0204 | - 0.0170 | 0.975 |
| | R | 0.00128 | 0.0222 | - 0.0308 | 0.357 |
| | S | 0.00122 | 0.0227 | - 0.0399 | 0.356 |
| ( )[++] | | 0.00126 | 0.0231 | - 0.0513 | - |

[+] Values at nearest Gauss point

[++] Classical thin plate solution (Ref. 7).

4. T. J. R. Hughes, M. Cohen and M. Haroun, Reduced and selective integration techniques in the finite element analysis of plates. *Nucl. Engng Design* **46**, 203–222 (1978).
5. T. J. R. Hughes and M. Cohen, The "Heterosis" finite element for plate bending. *Comput. Structures* 9, 445–450 (1978).
6. R. D. Mindlin, Influence of rotary inertia and shear on flexural motions of isotopic elastic plates. *J. Appl. Mech.* **18**, 31–38 (1951).
7. S. P. Timoshenko and S. Woinowsky-Krieger, *Theory of Plates and Shells*. McGraw-Hill, New York (1959).
8. E. Reissner, On transverse bending of plates, including the effects of transverse shear deformation. *Int. J. Solids Structures* **11**, 569–573 (1975).
9. T. Kant, The segmentation method in the analysis of elastic plates with two opposite edges simply supported using a refined higher order theory. *Rep. C/R/366/80*. Department of Civil Engineering, University of Wales, Swansea SA2 8PP, 1980 (to be published).
10. O. C. Zienkiewicz, *The Finite Element Method*. McGraw-Hill, U.K. (1977).
11. Y. K. Cheung and M. F. Yeo, *A Practical Introduction to Finite Element Analysis*, pp. 94–96. Pitman, London (1979).
12. A. K. Noor and S. J. Hartley, Evaluation of element stiffness matrices on CDC STAR-100 computer. *Comput. Structures* 9, 151–161 (1978).
13. A. K. Gupta and B. Mohraz, A method of computing numerically integrated stiffness matrices. *Int. J. Num. Meth. Engng.* **5**, 83–89 (1972).
14. E. Hinton and D. R. J. Owen, *Finite Element Programming*. Academic Press, London (1977).
15. O. C. Zienkiewicz, R. L. Taylor and J. M. Too, Reduced integration techniques in general analysis of plates and shells. *Int. J. Num. Meth. Engng.* 3, 275–290 (1971).
16. O. C. Zienkiewicz and E. Hinton, Reduced integration, function smoothing and non-conformity in finite element analysis (with special reference to thick plates). *J. Franklin Inst.* **302**, 443–461 (1976).

### APPENDIX 1. ELEMENTS OF $[B_i^T D B_j]$ MATRIX.†

| | | | | | |
|---|---|---|---|---|---|
| 0 | 0 | 0 | 0 | 0 | 0 |
| 0 | $D_1(1-\nu)\frac{\partial N_i}{\partial x}\cdot\frac{\partial N_j}{\partial x} + \frac{D_1(1-2\nu)}{2}\frac{\partial N_i}{\partial y}\cdot\frac{\partial N_j}{\partial y}$ | $D_1\nu\frac{\partial N_i}{\partial x}\cdot\frac{\partial N_j}{\partial y} + \frac{D_1(1-2\nu)}{2}\frac{\partial N_i}{\partial y}\cdot\frac{\partial N_j}{\partial x}$ | $2D_1\nu\frac{\partial N_i}{\partial x}N_j$ | $D_1^*(1-\nu)\frac{\partial N_i}{\partial x}\cdot\frac{\partial N_j}{\partial x} + \frac{D_1^*(1-2\nu)}{2}\frac{\partial N_i}{\partial y}\cdot\frac{\partial N_j}{\partial y}$ | $D_1^*\nu\frac{\partial N_i}{\partial x}\cdot\frac{\partial N_j}{\partial y} + \frac{D_1^*(1-2\nu)}{2}\frac{\partial N_i}{\partial y}\cdot\frac{\partial N_j}{\partial x}$ |
| 0 | $D_1\nu\frac{\partial N_i}{\partial y}\cdot\frac{\partial N_j}{\partial x} + \frac{D_1(1-2\nu)}{2}\frac{\partial N_i}{\partial x}\cdot\frac{\partial N_j}{\partial y}$ | $D_1(1-\nu)\frac{\partial N_i}{\partial y}\cdot\frac{\partial N_j}{\partial y} + \frac{D_1(1-2\nu)}{2}\frac{\partial N_i}{\partial x}\cdot\frac{\partial N_j}{\partial x}$ | $2D_1\nu\frac{\partial N_i}{\partial y}N_j$ | $D_1^*\nu\frac{\partial N_i}{\partial y}\cdot\frac{\partial N_j}{\partial x} + \frac{D_1^*(1-2\nu)}{2}\frac{\partial N_i}{\partial x}\cdot\frac{\partial N_j}{\partial y}$ | $D_1^*(1-\nu)\frac{\partial N_i}{\partial y}\cdot\frac{\partial N_j}{\partial y} + \frac{D_1^*(1-2\nu)}{2}\frac{\partial N_i}{\partial x}\cdot\frac{\partial N_j}{\partial x}$ |
| 0 | $2D_1\nu N_i\frac{\partial N_j}{\partial x}$ | $2D_1\nu N_i\frac{\partial N_j}{\partial y}$ | $4D_1(1-\nu)N_iN_j$ | $2D_1^*\nu N_i\frac{\partial N_j}{\partial x}$ | $2D_1^*\nu N_i\frac{\partial N_j}{\partial y}$ |
| 0 | $D_1^*(1-\nu)\frac{\partial N_i}{\partial x}\cdot\frac{\partial N_j}{\partial x} + \frac{D_1^*(1-2\nu)}{2}\frac{\partial N_i}{\partial y}\cdot\frac{\partial N_j}{\partial y}$ | $D_1^*\nu\frac{\partial N_i}{\partial x}\cdot\frac{\partial N_j}{\partial y} + \frac{D_1^*(1-2\nu)}{2}\frac{\partial N_i}{\partial y}\cdot\frac{\partial N_j}{\partial x}$ | $2D_1^*\nu\frac{\partial N_i}{\partial x}N_j$ | $D_1^{**}(1-\nu)\frac{\partial N_i}{\partial x}\cdot\frac{\partial N_j}{\partial x} + \frac{D_1^{**}(1-2\nu)}{2}\frac{\partial N_i}{\partial y}\cdot\frac{\partial N_j}{\partial y}$ | $D_1^{**}\nu\frac{\partial N_i}{\partial x}\cdot\frac{\partial N_j}{\partial y} + \frac{D_1^{**}(1-2\nu)}{2}\frac{\partial N_i}{\partial y}\cdot\frac{\partial N_j}{\partial x}$ |
| 0 | $D_1^*\nu\frac{\partial N_i}{\partial y}\cdot\frac{\partial N_j}{\partial x} + \frac{D_1^*(1-2\nu)}{2}\frac{\partial N_i}{\partial x}\cdot\frac{\partial N_j}{\partial y}$ | $D_1^*(1-\nu)\frac{\partial N_i}{\partial y}\cdot\frac{\partial N_j}{\partial y} + \frac{D_1^*(1-2\nu)}{2}\frac{\partial N_i}{\partial x}\cdot\frac{\partial N_j}{\partial x}$ | $2D_1^*\nu\frac{\partial N_i}{\partial y}N_j$ | $D_1^{**}\nu\frac{\partial N_i}{\partial y}\cdot\frac{\partial N_j}{\partial x} + \frac{D_1^{**}(1-2\nu)}{2}\frac{\partial N_i}{\partial x}\cdot\frac{\partial N_j}{\partial y}$ | $D_1^{**}(1-\nu)\frac{\partial N_i}{\partial y}\cdot\frac{\partial N_j}{\partial y} + \frac{D_1^{**}(1-2\nu)}{2}\frac{\partial N_i}{\partial x}\cdot\frac{\partial N_j}{\partial x}$ |

(a) Flexure contribution.

| | | | | | |
|---|---|---|---|---|---|
| $\frac{K_1(1-2\nu)}{2}\left(\frac{\partial N_i}{\partial x}\cdot\frac{\partial N_j}{\partial x} + \frac{\partial N_i}{\partial y}\cdot\frac{\partial N_j}{\partial y}\right)$ | $\frac{K_1(1-2\nu)}{2}\frac{\partial N_i}{\partial x}\cdot N_j$ | $\frac{K_1(1-2\nu)}{2}\frac{\partial N_i}{\partial y}\cdot N_j$ | $\frac{D_1(1-2\nu)}{2}\left(\frac{\partial N_i}{\partial x}\cdot\frac{\partial N_j}{\partial x} + \frac{\partial N_i}{\partial y}\cdot\frac{\partial N_j}{\partial y}\right)$ | $\frac{3}{2}D_1(1-2\nu)\frac{\partial N_i}{\partial x}\cdot N_j$ | $\frac{3}{2}D_1(1-2\nu)\frac{\partial N_i}{\partial y}\cdot N_j$ |
| $\frac{K_1(1-2\nu)}{2}N_i\frac{\partial N_j}{\partial x}$ | $\frac{K_1(1-2\nu)}{2}N_iN_j$ | 0 | $\frac{D_1(1-2\nu)}{2}N_i\frac{\partial N_j}{\partial x}$ | $\frac{3}{2}D_1(1-2\nu)N_iN_j$ | 0 |
| $\frac{K_1(1-2\nu)}{2}N_i\frac{\partial N_j}{\partial y}$ | 0 | $\frac{K_1(1-2\nu)}{2}N_iN_j$ | $\frac{D_1(1-2\nu)}{2}N_i\cdot\frac{\partial N_j}{\partial y}$ | 0 | $\frac{3}{2}D_1(1-2\nu)N_iN_j$ |
| $\frac{D_1(1-2\nu)}{2}\left(\frac{\partial N_i}{\partial x}\cdot\frac{\partial N_j}{\partial x} + \frac{\partial N_i}{\partial y}\cdot\frac{\partial N_j}{\partial y}\right)$ | $\frac{D_1(1-2\nu)}{2}\frac{\partial N_i}{\partial x}\cdot N_j$ | $\frac{D_1(1-2\nu)}{2}\frac{\partial N_i}{\partial y}\cdot N_j$ | $\frac{D_1^*(1-2\nu)}{2}\left(\frac{\partial N_i}{\partial x}\cdot\frac{\partial N_j}{\partial x} + \frac{\partial N_i}{\partial y}\cdot\frac{\partial N_j}{\partial y}\right)$ | $\frac{3}{2}D_1^*(1-2\nu)\frac{\partial N_i}{\partial x}\cdot N_j$ | $\frac{3}{2}D_1^*(1-2\nu)\frac{\partial N_i}{\partial y}\cdot N_j$ |
| $\frac{3}{2}D_1(1-2\nu)N_i\frac{\partial N_j}{\partial x}$ | $\frac{3}{2}D_1(1-2\nu)N_iN_j$ | 0 | $\frac{3}{2}D_1^*(1-2\nu)N_i\frac{\partial N_j}{\partial x}$ | $\frac{9}{2}D_1^*(1-2\nu)N_iN_j$ | 0 |
| $\frac{3}{2}D_1(1-2\nu)N_i\frac{\partial N_j}{\partial y}$ | 0 | $\frac{3}{2}D_1(1-2\nu)N_iN_j$ | $\frac{3}{2}D_1^*(1-2\nu)N_i\frac{\partial N_j}{\partial y}$ | 0 | $\frac{9}{2}D_1^*(1-2\nu)N_iN_j$ |

(b) Transverse shear contribution.

† $K_1 = Eh/(1+\nu)(1-2\nu)$, $D_1 = K_1h^2/12$, $D_1^* = 3D_1h^2/20$, $D_1^{**} = 5D_1^*h^2/28$.